Asymmetric color matching: how color appearance depends on the illuminant

David H. Brainard* and Brian A. Wandell

Department of Psychology, Stanford University, Stanford, California 94305

Received June 10, 1991; revised manuscript received February 19, 1992; accepted February 20, 1992

We report the results of matching experiments designed to study the color appearance of objects rendered under different simulated illuminants on a CRT monitor. Subjects set asymmetric color matches between a standard object and a test object that were rendered under illuminants with different spectral power distributions. For any illuminant change, we found that the mapping between the cone coordinates of matching standard and test objects was well approximated by a diagonal linear transformation. In this sense, our results are consistent with von Kries's hypothesis {Handb. Physiol. Menschen **3**, 109 (1905) [in *Sources of Color Vision*, D. L. MacAdam, ed. (MIT Press, Cambridge, Mass., 1970)]} that adaptation simply changes the relative sensitivity of the different cone classes. In addition, we examined the dependence of the diagonal transformation on the illuminant change. For the range of illuminants tested, we found that the change in the diagonal elements of the linear transformation was a linear function of the illuminant change.

INTRODUCTION

We report the results from a set of experiments designed to study how the color appearance of objects depends on the illuminant. To measure appearance, we used an asymmetric color-matching procedure. In the basic color-matching experiment a subject equates the appearances of two lights presented in a common context. Asymmetric color matching generalizes basic color matching by permitting the lights to be presented in different visual contexts. The subject adjusts the appearance of a test light, presented in one visual context, to match the appearance of an experimentally controlled standard light, presented in a second visual context.

Our stimuli were CRT simulations of flat objects rendered under diffuse illumination. The subjects set asymmetric color matches between a standard object and a test object that were rendered under illuminants with different spectral power distributions. Because the visual system adapts in response to illumination changes, our asymmetric color matches were not photopigment absorption matches. Rather, our experiments measured neural equivalencies at a later point in the visual pathways.[1]

Asymmetric matches provide the empirical measurements for a theory of color appearance that describes how the visual system adapts to changes in illumination. The matches establish equivalent appearances across illuminations. A complete theory of asymmetric color matching must include two parts[2]: First, the theory should describe the functional form of the transformation that relates the standard and the test objects' cone coordinates. Second, the theory should describe how the parameters of the transformation depend on the illuminants.

We examined our data for regularities in the functional form of the mapping between the cone coordinates of the standard and the test objects. For each illuminant change we examined, we found that this mapping was well approximated by a diagonal linear transformation. In this sense, our data are consistent with von Kries's[3] hypothesis that adaptation simply changes the relative sensitivity of the different cone classes. We went on to examine how the diagonal elements of the linear transformation depend on the illuminant change. Here again we found a simple linear relationship. Taken together, these two regularities imply that data from a small number of experimental conditions can be used to predict the dependence of color appearance on a wide range of illumination changes.

METHODS OVERVIEW

The subjects began each session with a training period during which they learned the color appearance of a standard object rendered under a standard illuminant. After the training period, the subjects set the color appearance of a test object to match the color appearance of the standard object. Since the standard object was no longer visible, our procedure required the subjects to remember the appearance of the standard object. The test object and its complex surround were rendered either under the standard illuminant or under a test illuminant. Symmetric matches set under the standard illuminant served to establish the precision to which the subjects could set memory matches. Asymmetric matches set under six test illuminants provided the main experimental data.

Our visual stimuli were presented on a CRT monitor. The stimulus was always a simulation of an array of flat matte objects rendered under spatially uniform illumination, as shown in Fig. 1. One of the objects in the array was the test object. The subjects pressed buttons to adjust the appearance of the test object. We fixed the simulated illuminant while the subjects set each individual match. During the matching process, however, we changed the position of the test object in the array and changed the identity of the objects that made up the test object's surround. Between matches we changed the illuminant gradually over a 2-min period. We discuss the rationale for several aspects of the experimental design in the following subsections.

0740-3232/92/091433-16$05.00

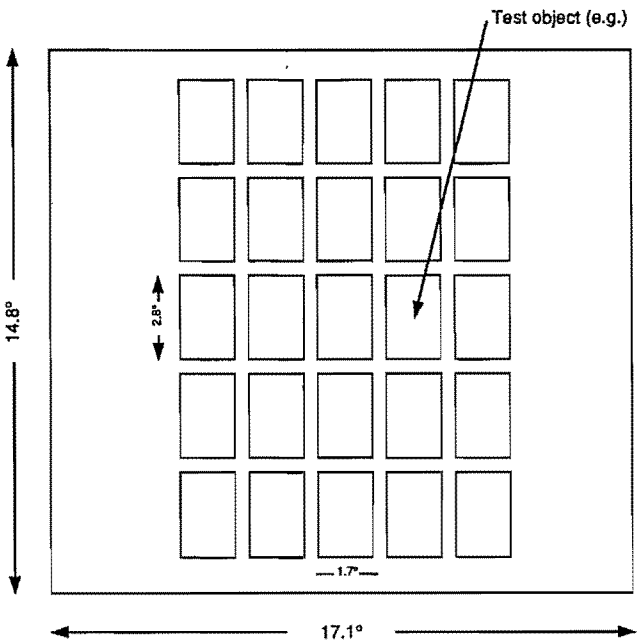

Fig. 1. Visual stimulus. The subjects saw CRT simulations of a collection of flat matte surfaces rendered under spatially uniform illumination. One of the surfaces in the array was the test object. A detailed description of the stimulus is given in the Methods section. The dimensions specified in the figure are degrees of visual angle.

Stimulus Configuration

At present, bringing all the richness of natural images into the laboratory would make the construction, manipulation, and description of the experimental stimuli intractable. We designed our stimuli to be as simple as possible while still incorporating enough spectral information so that a trichromatic observer could correctly estimate the illuminant. We constrained our simulated object surface reflectance functions and illuminant spectral power distributions to be drawn from small-dimensional linear models. These models provide a good description of the class of naturally occurring surfaces and illuminants.[4-8] Buchsbaum[9] and Maloney and Wandell[10] have presented algorithms that correctly estimate the illuminant spectral power distribution when spectral constraints of this type hold. In addition to the spectral constraints, the algorithms require that the image contain multiple objects sharing a common illuminant. For this reason our stimulus consisted of a simulation of an array of uniformly illuminated objects. We have confirmed that the algorithm of Buchsbaum accurately recovers the illuminant when it is run on our stimuli.[11] A stimulus consisting of a test on a uniform background does not contain enough information for a trichromatic observer to estimate the illuminant, since changes in the spectral properties of the background can be due to changes in the spectral power distribution of the illuminant or changes in the surface reflectance of the background object.

Changing Test Location and Object Identity during Matches

The subjects adjusted the appearance of the test object by pressing buttons. After each button press, we randomized the location of the test object and the identity of the simulated objects, using a procedure described in detail below (see Methods). Through this randomization, we hoped to isolate the effect of changing the illuminant from the effects of other variables on color appearance, such as the identity of neighboring objects.

A second rationale for the randomization was to prevent the subjects from using the appearance of a fixed object as a reference to identify changes in the simulated illuminant. In an experiment that used stimuli similar to ours but without object randomization, Arend and Reeves[12] demonstrated that subjects have access to multiple strategies for setting asymmetric color matches. We believe that reasoning about object identity mediated performance for some of their conditions. How well subjects can perform such reasoning tasks is an interesting question in its own right, but it is a different question from that of how color appearance depends on viewing context.

Time Course of Illuminant Changes

We believe that it is important to have the subject's state of adaptation under experimental control. Our use of a memory-matching procedure allowed us to control adaptation because the subject did not have to view the test and the standard viewing contexts simultaneously. Simulated illuminant changes took place only between matches. The subjects spent approximately 1 min adjusting the appearance of the test object for each memory match. While they set the match, we held the simulated illuminant constant.

Measurements of the time course of adaptation show that it requires tens of seconds or even minutes for color appearance to stabilize after a change in viewing context.[13-17] Helson and others insisted on careful control of adaptation as part of their experimental designs.[18-23] In many recent experiments designed to study the effect of changing the illuminant, temporal variation of the illuminant was not under experimental control. The subjects were free to move their eyes about between a pair of images with different illuminants, which prevented the subjects from reaching a steady adapted state.[12,24-28] Procedural differences in the control of adaptation can lead to different empirical results.

Use of Simulations

Our stimuli were simulations of physical objects and illuminants presented on a calibrated CRT.[29] Simulation offers advantages in controlling the temporal and spatial structure of the stimuli. For example, randomization of the objects would be difficult to achieve with stimuli consisting of real objects and illuminants. On the other hand, the use of a CRT raises the question of whether the visual system processes simulated and real images in the same way.

Our current understanding of the initial encoding of light by the visual system provides a firm theoretical foundation for the use of CRT simulations: the simulated images were designed to generate the same responses from the retinal cone mosaic as the reflectance images they simulate. Many factors limit the precision with which simulations can control the retinal image. These include the discrete spatial resolution of the display, the finite precision of the monitor calibration, the role of rods in color vision at the near-mesopic light levels produced by the

monitor, and variations in color-matching functions between individuals, with eccentricity, and with field size. Even with these limitations, we believe that the simulations provide a reasonable visual match to the reflectance images that they were designed to replace.[30]

Monitor simulations are but one of many laboratory simplifications and probably not the most important. The objects we simulate consist of flat matte surfaces rendered under spatially uniform illumination and presented in an otherwise dark room. Our stimuli are thus quite different from most natural images. As we learn to conduct experiments using larger images containing textures, three-dimensional objects, shadows, and so forth, we are likely to discover principles beyond those revealed in the present experiments. Our stimuli are a compromise. They are richer than the traditional disk-on-background stimuli, and they contain sufficient information to allow the visual system to process them as reflectance images.

METHODS

The visual display consisted of 25 small rectangular foreground regions against a large background region, as illustrated in Fig. 1. The foreground regions subtended 2.8° × 1.7° of visual angle vertically and horizontally, respectively, and they were separated by 0.1° vertically and 0.06° horizontally. The background region subtended 14.8° × 17.1° of visual angle vertically and horizontally, respectively. We presented the simulated images on a computer-controlled color monitor (Barco Model 5351) in an otherwise dark room. The subjects viewed the screen without head restraint from a distance of 105 cm. The video input to the monitor was generated by a frame buffer (Number Nine Graphics Corp. Model 232808) that in turn was controlled by a computer (IBM Model PC-XT, modified to use an 8086 microprocessor). The frame buffer provided a precision of 8 bits per pixel per phosphor and was configured to generate a monitor image 640 pixels wide by 350 pixels high at a refresh rate of 87 full frames per second (noninterlaced).

We calibrated the monitor's phosphor spectral power distributions and the nonlinear relationship between the frame-buffer values and phosphor intensities. Brainard[29] describes the calibration measurements in detail and presents the model of monitor performance that was used to determine this relation. The luminance of the monitor white point, where all three phosphors contributed maximally, was 70 cd/m^2.

To simulate a given object under a given illuminant, we multiplied the surface reflectance function and the illuminant spectral power distribution. This product is the spectral power distribution of the reflected light. We computed the CIE XYZ tristimulus coordinates of this reflected light and set values in the monitor frame buffer so that the emitted color signal had the same CIE XYZ tristimulus coordinates. The simulation computations were performed during the experimental sessions, using the data representations and subroutine libraries provided by the Stanford Color Analysis Package.[31,32]

The simulated surface reflectances in the foreground region were chosen from a list of 226 reflectances. These were a subset of 462 Munsell paper reflectance functions measured by Kelly *et al.*[33,34] There is some evidence that the reflectance functions of the Munsell papers are representative of naturally occurring surface reflectance functions.[5,7] We selected the smaller list of reflectances by determining which could be simulated within the monitor gamut under all our simulated illuminants. The simulated surface reflectances in the background region were chosen from a list of 12 dark reflectances. We restricted the background objects to be dark because in pilot studies we found changes between bright background objects to be visually jarring. The full reflectance functions of the simulated objects are provided in Brainard's dissertation.[35] The gamut of these reflectances is shown in Fig. 7 below.

Cohen and others have shown that the reflectance functions of the Munsell papers are well described by a small-dimensional linear model.[4-6] For computational convenience, we approximated the measured functions with respect to a six-dimensional linear model whose basis functions were the first six principal components of the entire data set of Kelly *et al.*[33,34]

We used 19 different standard objects in our experiments. The cone coordinates (see below) of the standard objects rendered under the standard illuminant are tabulated in Appendix B.

The simulated illuminants in our experiments were typical of natural daylight. We used seven different illuminants, all of which were constructed from a two-dimensional linear model whose basis functions were the mean and first characteristic function of a large number of measured daylight spectra.[8] The spectral power distributions of the seven illuminants are plotted in Fig. 2.

We held the standard illuminant fixed in the experiments reported here. It always had the spectral power distribution of illuminant S of Fig. 2. Illuminants T1–T6 were used as test illuminants. The spectral properties of the illuminants are provided in Appendix B.

Experimental Control of Color Appearance

The subjects pressed buttons to control the test object's coordinates in the CIELUV uniform color space. The CIELUV color space was designed so that Euclidean distance in the space corresponds roughly to perceptual difference.[36,37] Using equal steps in this space proved a convenient way to make the perceptual effects of button presses approximately the same, independent of the adjusted object's current cone coordinates.[38] One button was assigned to each of the three CIELUV coordinates L^*, u^*, and v^*. The subject could increase or decrease the adjusted lights' L^*, u^*, and v^* coordinates in discrete adjustment steps. The L^* steps were always 4 units, while the u^* and v^* steps were always 5 units. The subject's adjustments were constrained to lie within a rectangular solid in the CIELUV color space. The L^*, u^*, and v^* dimensions of this solid were 36, 45, and 45 units, respectively. The L^*, u^*, or v^* coordinate was randomized if the subject attempted to adjust the test object past the boundaries of the constraining region.

Both the simulated objects and the location of the test object changed after each button press. First, the reflectances of 10 of the 25 simulated objects were replaced by random draw from the list of 226 possible reflectances. This replacement schedule ensured that, while making the adjustment, the subject saw the test object in many different contexts that shared a common simulated illuminant

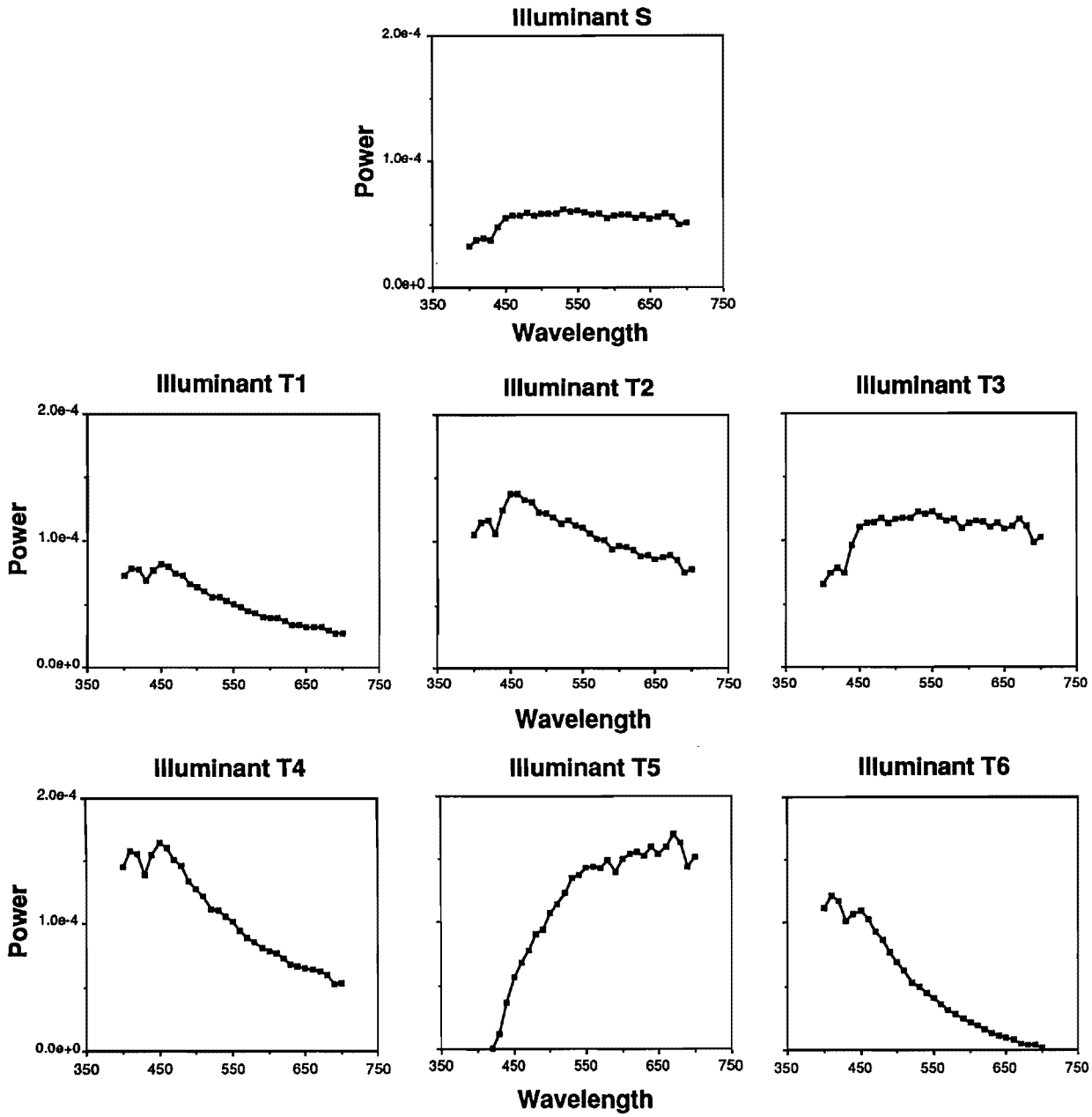

Fig. 2. Experimental illuminants. Each panel shows the spectral power distribution of one experimental illuminant. The standard illuminant in all our conditions was illuminant S. Illuminants T1–T6 were used as test illuminants. The units of power are milliwatts per square centimeter nanometer steradian.

and that no particular object was present during the entire matching process. Second, the simulated object in the background region was replaced by random draw from the list of 12 possible background reflectances with a probability of 0.25. Changing ten objects rather than all and only occasionally changing the background object made the changes less jarring. Third, the location of the test object was selected at random from the 25 possible foreground regions. The position of the test object was indicated by a small whitish rectangle flashed at the center of the foreground location that contained the light being adjusted. We found in pilot studies that changing the test object location was critical to the subject's ability to set the color appearance matches. Using a fixed location introduced strong local adaptation effects.

Procedure

The subject began an experimental session by viewing a sequence of images containing the standard object amid an array of simulated objects. From one image to the next, we randomized the objects in the array and the location of the standard object, as described above. We call the simulated illuminant during initial viewing the standard illuminant.

After the initial viewing, the subject set a series of appearance matches. The experiment proceeded by alternating four training and four experimental phases. In a training phase we rendered the array of objects with the standard illuminant. The subject set three matches to the standard object. He or she received feedback about the accuracy of the match. A single tone indicated that the

match was within one adjustment step (4 or 5 ΔE_{uv}^* units) of the standard object, and two tones indicated that the match was more than one step from the standard object. After the feedback was given, the subject was shown the standard object.

In each of the four experimental phases the subject also set three matches, but no feedback was given. In two of the experimental phases we rendered the objects with the standard illuminant, and in the other two we rendered the objects with a test illuminant. The presentation order of the two types of test phase was randomized for each session.

Between each training and experimental phase the subject saw a sequence of 120 images, presented at a rate of 1/s. Changes between the standard illuminant and the test illuminant took place gradually during this interval, and the identity of the simulated objects was randomized from image to image.

Subjects observed in experimental sessions that lasted ~1 h. Only one standard object and one test illuminant were used in a single session. The subjects always ran two sessions for an experimental condition, which was defined by the standard object and the test illuminant. Thus for each experimental condition we obtained 12 (3 matches/phase × 2 phases/session × 2 sessions) symmetric matches from the test phases when there was no illuminant change and 12 asymmetric matches when the illuminant was changed. The symmetric matches measured how accurately the subjects performed the memory matching task. The asymmetric matches measured the effect of the illuminant change on color appearance.

The experimental procedure also included a classification task, which was interleaved with the matching task. We do not discuss the classification data in this paper.

Subjects

One of the authors (DB, male, 18 conditions), a paid graduate student (KH, male, 9 conditions), and three paid undergraduates (SE, male, 27 conditions; DW, female, 3 conditions; LL, female, 4 conditions) participated in the experiments reported here. All had normal color vision as tested with the Ishihara color plates.[39] The bulk of the observations were performed by DB and SE. Subject DB was an experienced psychophysical observer and was aware of the design and purpose of the experiments. Subject SE was naïve but became progressively better informed about the experiment over several months of observing. Subjects KH, LL, and DW were naïve and remained so. Their results served to confirm the data obtained by DB and SE.

Before participating in the experiments, the subjects took part in approximately 6 h of practice sessions. During these sessions, no illuminant change was introduced. Two other subjects (paid undergraduates) were unable to learn the experimental procedure or to set reliable memory matches and did not participate further.

Our data set includes 732 individual asymmetric color matches from five subjects set in a total of 61 experimental conditions. These conditions include some replications both within and between subjects. The data are tabulated in Appendix B.

Data Analysis

Our models of the illuminant's effect on color appearance are formulated to relate the L, M, and S (long-, medium-, and short-wavelength-sensitive, respectively) cone coordinates of the standard object rendered under the standard illuminant to the cone coordinates of the asymmetric match. Our cone coordinates are proportional to cone photopigment quantal absorption rates. To compute cone coordinates, we used the Smith–Pokorny[40] estimates of the cone photopigment spectral responsivities corrected for preretinal absorptions.[40–44]

In the basic color-matching experiment, the distribution of individual color matches in cone coordinates or CIE XYZ tristimulus coordinates is known to be ellipsoidal and to depend on the coordinates of the standard object.[45–47] These representations do not provide a perceptual metric for the experimental variability of color matches. We believe that it is inappropriate to evaluate the precision of our experimental procedure or the quality of our model fits by using a distance measure that is based directly on either of these representations. Therefore we convert our data to the CIELUV uniform color and use the CIELUV metric, ΔE_{uv}^*, to evaluate the size of errors.[48]

If the distributions of the match L^*, u^*, and v^* coordinates are normal, independent, and identically distributed, then we can compute the radius of a 90% confidence sphere for the mean matches. The probability that the true match falls within the volume of the confidence sphere is 0.90. We computed the confidence sphere by using standard theorems about distributions of distances for samples of multivariate normal distributions.[49] The radius of the confidence sphere was 3.18 ΔE_{uv}^* units both for the symmetric matches (no illuminant change) and for the asymmetric matches (illuminant change). The subjects set their memory matches with the same precision whether the illuminant changed or not.

The mean distance between the standard object and the mean match in the symmetric case was 5.02 ΔE_{uv}^* units. Thus in general the standard object fell outside the confidence sphere of the mean match by a small amount.[50] We observed no significant differences in the performance of our individual subjects.[51] In our evaluation of models, we pooled the data from all our subjects.

RESULTS

The independent variables of an experimental condition are the standard object, the standard illuminant, and the test illuminant. The dependent variable is the mean asymmetric color match. We represent the standard object by its cone coordinates when it is rendered under the standard illuminant. The standard illuminant was held fixed throughout the experiments reported here, and we do not represent it explicitly in our formulation. We represent the test illuminant by how much it differs from the standard illuminant, and we call this difference the illuminant change. Thus the explicit independent variables are the standard object and the illuminant change. We represent the mean asymmetric matches by the difference between the cone coordinates of the matching test object (rendered under the test illuminant) and those of the standard object (rendered under the standard illuminant). We

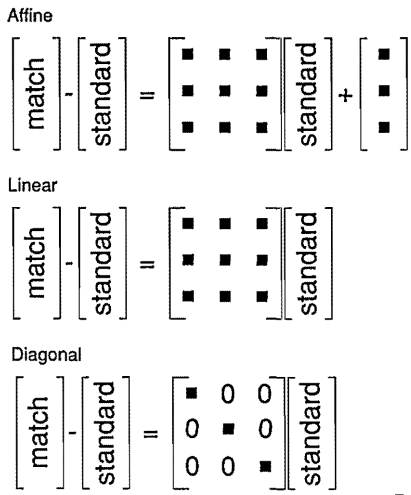

Fig. 3. Transformation models. The match change is illustrated by the vector differences on the left-hand side of each panel. For a fixed illuminant change, each of the models uses a different functional form for the transformation between the standard object's cone coordinates and the match change. Each panel illustrates this functional form for one of our models. The filled squares illustrate matrix and vector elements that can vary with the illuminant change.

$$\begin{bmatrix} a+u & 0 & 0 \\ 0 & b+v & 0 \\ 0 & 0 & c+w \end{bmatrix} = \begin{bmatrix} a & 0 & 0 \\ 0 & b & 0 \\ 0 & 0 & c \end{bmatrix} + \begin{bmatrix} u & 0 & 0 \\ 0 & v & 0 \\ 0 & 0 & w \end{bmatrix}$$

Fig. 4. Illuminant linearity. Illuminant linearity means that the transformation parameters are linear functions of the illuminant change. This property implies that the transformation for the sum of two illuminant changes is given by the sum of the transformations for each illuminant change alone. The figure illustrates illuminant linearity for the diagonal model. As noted in the text, the illuminant linearity property holds with respect to a fixed standard illuminant. In Appendix A we describe how our models may be generalized to handle the case in which the standard illuminant is permitted to vary.

call this difference the match change. The match change can be used together with the standard object's cone coordinates to recover the asymmetric match.

We present our results by testing three models of the effect of the illuminant change on subjects' asymmetric matches. The models are illustrated in Figs. 3 and 4. The match change is illustrated by the vector differences at the left of Fig. 3. The elements of these three-dimensional vectors specify the L, M, and S cone coordinates. For a fixed illuminant change, each of the models uses a different functional form for the transformation between the standard object's cone coordinate vector and the match change. In the most general model, the affine model, the transformation is a matrix multiplication plus an added vector. The values of the matrix and the vector depend on the illuminant change. The affine model generalizes the two-process model proposed by Jameson and Hurvich.[52,53] The model is consistent with a large body of data collected by using isolated tests presented on uniform backgrounds or annuli.[23,54-56] The linear model is a special case of the affine model in which the added vector is zero. The diagonal model is a special case of the linear model in which the matrix is diagonal. The diagonal transformation is often referred to as von Kries adaptation, since changes in the diagonal elements of the matrix represent changes in the relative sensitivities of the three cone classes.[3]

We collected data for six different illuminant changes. In addition to describing the functional form of the transformation, a complete theory should describe how the parameters of the transformation depend on the illuminant change. In all three models we assume that the transformation parameters are linear functions of the illuminant change. We call this property illuminant linearity. Figure 4 illustrates illuminant linearity for the diagonal model. Our motivation for testing illuminant linearity was derived from a computational analysis of the physics of reflectance.[11,35] Color-constant systems that represent color appearance by an estimate of surface reflectance exhibit illuminant linearity. Illuminant linearity is also consistent with a strong form of von Kries adaptation in which the gain of each cone class is assumed to be inversely proportional to some spatial and temporal average of the quantal absorptions for that class (see Appendix A).

It is worth emphasizing two features of our models here. First, we formulated the models to predict the cone coordinates of the match change rather than the cone coordinates of the asymmetric match. This choice is important because it greatly simplifies the formal expression of the illuminant linearity property. Second, we formulated the models to apply only to the case in which the standard illuminant is held fixed. For this reason, the standard illuminant does not appear explicitly as an independent variable in the formulation. In Appendix A we present a formal description of our models and develop a natural generalization to handle the case in which the standard illuminant is permitted to vary.

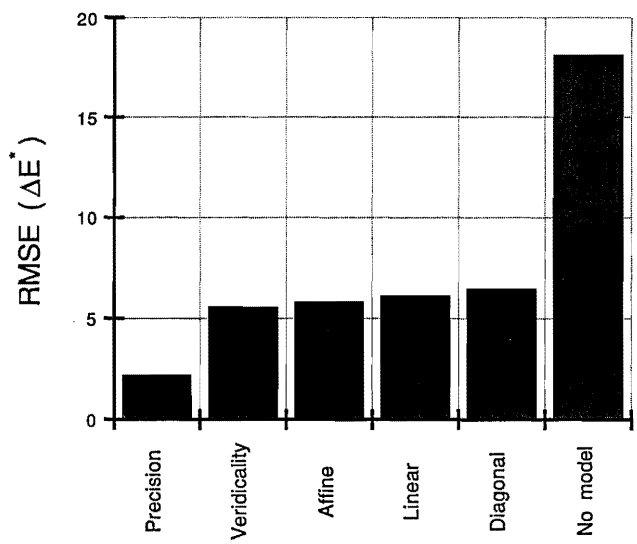

Fig. 5. Quality of model fit. The vertical axis shows the rms error in ΔE_{uv}^* values. The first bar (precision) shows the rms deviation of individual matches about the mean match. The variability of the symmetric and the asymmetric matching conditions was about the same, and the conditions are grouped to form this estimate. The second bar (veridicality) shows the rms deviation between the mean symmetric matches and the standard object. The next three bars (affine, linear, diagonal) show the rms ΔE_{uv}^* errors for the three models' predictions of the asymmetric matches. The last bar (no model) shows the rms error of using the unmodified cone coordinates of the standard object under the standard illuminant to predict the cone coordinates of the asymmetric color match.

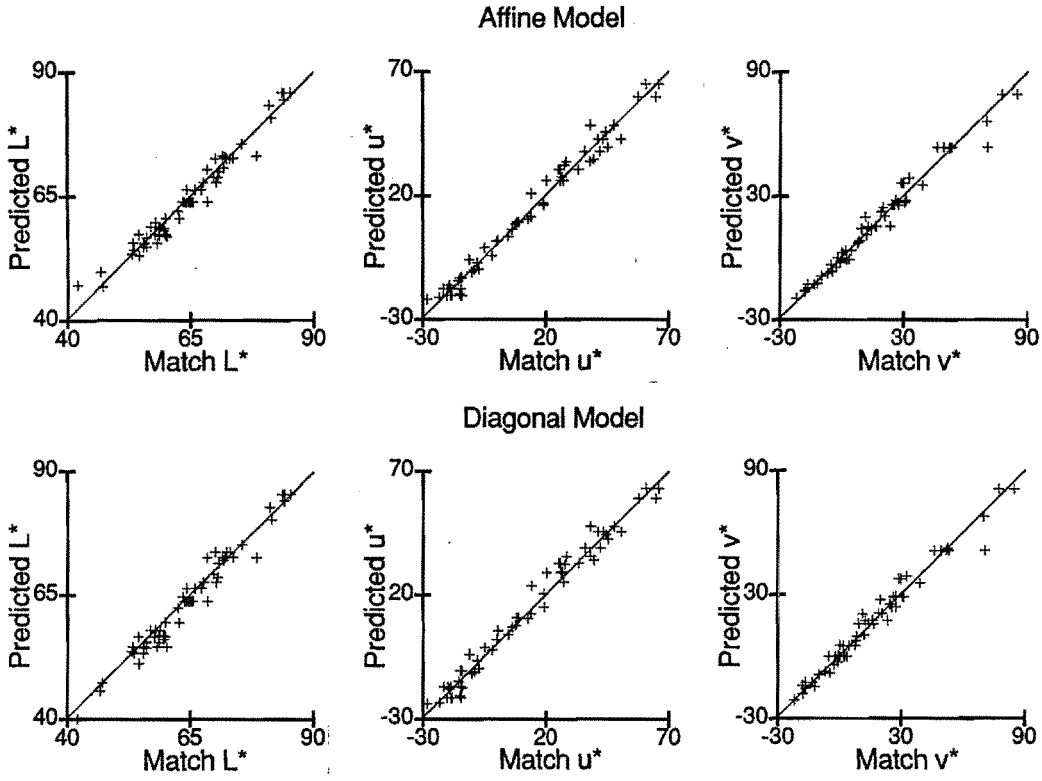

Fig. 6. Scatterplot of predicted matches versus measured mean asymmetric matches. Each panel shows a scatterplot for one of the CIELUV L^*, u^*, or v^* coordinates.

We fitted the mean matches across all the experimental conditions and subjects with each of the three models. Brainard[35] describes a procedure for fitting models that satisfy illuminant linearity. His procedure is based on multiple regression and minimizes the mean-square difference between the predicted and the measured match change. As described in Appendix A, we extended Brainard's procedure by using the STEPIT parameter search program[57] to minimize the mean-square CIELUV ΔE_{uv}^* difference between the predicted and the measured asymmetric matches. Because we used test illuminants that are described by a two-dimensional linear model, the affine model requires 24 (12 × 2) parameters, the linear model requires 18 (9 × 2) parameters, and the diagonal model requires 6 (3 × 2) parameters.

Figure 5 summarizes the quality of the model predictions in terms of the CIELUV ΔE_{uv}^* metric. Starting at the left, the first two bars define the precision of the matching procedure. The first bar (precision) shows the rms deviation of individual matches about the mean match. This bar defines the precision with which the subjects set the memory matches. The variability of the symmetric and the asymmetric matches was similar, and the two types of match were grouped to form this estimate.

The second bar (veridicality) shows the rms deviation between the mean symmetric matches and the standard object. This bar defines the precision with which the subjects remembered the color appearance of the standard object. The second bar is larger than the first, revealing that the symmetric memory matches were in general different from the standard object. We examined the errors across all the standard objects and illuminant changes and found that the only pattern visible in the deviations was a slight negative correlation ($r = -0.36$, $n = 61$) between the L^* coordinate of the standard object and the L^* deviation. The subjects tended to remember dark objects as being a little lighter and light objects as being a little darker.

The next three bars (affine, linear, diagonal) show the rms ΔE_{uv}^* errors for the three models' predictions of the asymmetric matches. All three models predict the asymmetric color matches about as well as the standard object predicts the symmetric matches.

The last bar (no model) shows the rms error of using the unmodified cone coordinates of the standard object under the standard illuminant to predict the cone coordinates of the asymmetric color match. This bar defines the size of the effect of changing the illuminant in our experiment.

Figure 6 compares the predicted and the observed mean matches for our entire data set under the affine and the diagonal models. Each panel of the figure shows the comparison for one CIELUV coordinate. If the models fitted perfectly, the data would lie along the diagonal of each panel. The data lie close to the diagonals for both models. The deviations of the points from the diagonals are the model residuals. The main difference in the model fits is a negative bias in L^* errors for the diagonal model. Because our three models are nested, the linear model (not shown) fits the data better than the diagonal model but not so well as the affine model.

All three models are based on the principle of illuminant linearity, and all provide a reasonable fit to the asymmetric color matches. We compared the nested sequence of models, using an F test. This test is based on the assumption that the CIELUV coordinates are independent and identically distributed. The data are powerful enough to reject both the linear and the diagonal models in favor of the affine model, at the 0.001 level. The difference be-

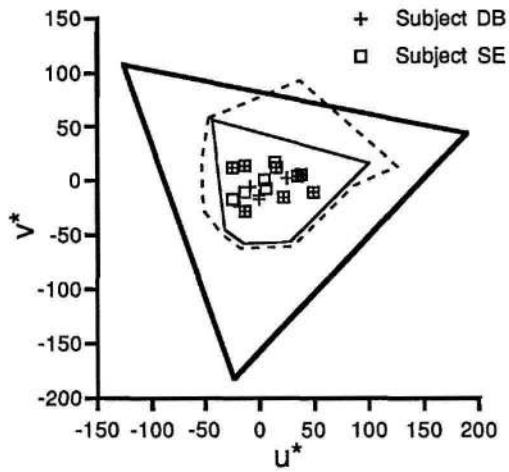

Fig. 7. CIELUV u^* and v^* chromaticity coordinates of the standard objects used for examining the functional form of the transformation. The coordinates were computed when the objects were rendered under the standard illuminant. Not apparent in the figure is the fact that the L^* coordinates of the objects also varied. For comparison, the solid polygon surrounding the points shows the gamut of all the surfaces measured by Kelly *et al.*[33,34] that could be simulated within our monitor gamut under all seven experimental illuminants. The gamut was computed by rendering the surfaces with our standard illuminant. The dashed polygon shows the gamut of the entire data set of Kelly *et al.* The triangle connects the CIELUV u^* and v^* coordinates of our three monitor phosphors.

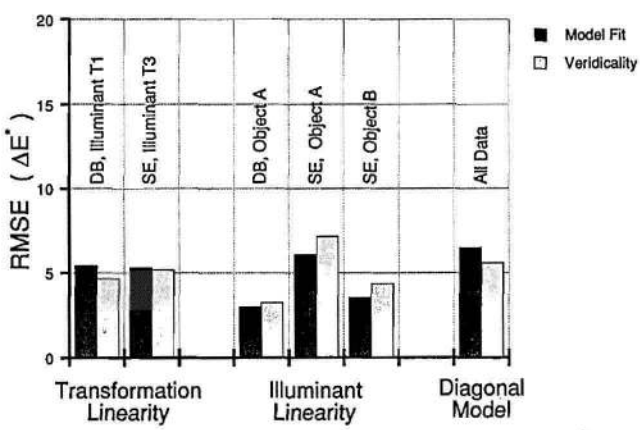

Fig. 8. Each pair of bars compares the rms error for model predictions to asymmetric matches for a data subset with the rms difference between the standard object and the symmetric match for the same data subset. The first two sets of bars evaluate the diagonal transformation when the illuminant change is held fixed. The middle sets of bars evaluate illuminant linearity when the standard object is held fixed. The last set of bars is replotted from the second and the fifth bars of Fig. 5 for comparison and evaluates the quality of the full diagonal model for the entire data set. The text above each bar identifies the data subset with reference to Appendix B.

tween the rms ΔE_{uv}^* error of the diagonal and the affine models is only 0.65 unit, however. We believe that this is too small to be of any practical significance. Appendix B provides the parameters of the diagonal model that provided the best fit to our data set.

Functional Form of the Transformation

We can examine the functional form of the transformation independently from the principle of illuminant linearity. Each of our main subjects made asymmetric matches for a large collection of standard objects and one illuminant change. Subject DB collected data for 13 standard objects with test illuminant T1, and subject SE collected data for 13 standard objects with test illuminant T3. The CIELUV u^* and v^* coordinates of the standard objects are plotted in Fig. 7.

When the illuminant change is held constant, we can evaluate the transformation without making assumptions about the dependence of the parameters on the illuminant change. The first two pairs of bars of Fig. 8 evaluate the quality of the diagonal transformation for the two data subsets when the illuminant change is held fixed. The diagonal model predicts the mean asymmetric matches as well as the standard object predicts the symmetric matches for both data sets.

Illuminant Linearity

We can also examine illuminant linearity independent of assumptions about the functional form of the transformation. Suppose that we fix the standard object and measure the change in match cone coordinates, using two different illuminant changes. Illuminant linearity predicts that, when we make a measurement for the sum of the illuminant changes, the measured match must be predicted by the sum of the match changes measured for each illuminant change alone.

We selected our illuminant changes to test illuminant linearity. The differences between the six test illuminants and the standard illuminants are all described as linear combinations of two basis illuminants. We can evaluate illuminant linearity by using data subsets in which the same standard object was used for all six illuminant changes. The three middle pairs of bars in Fig. 8 evaluate illuminant linearity when the standard object is held fixed. In each case illuminant linearity predicts the mean asymmetric matches as well as the standard object predicts the mean symmetric matches.

Use of CIELUV Space

We used the CIELUV coordinate space to fit our models and evaluate our prediction errors because this space was designed to make the distribution of the individual matches independent and identical. To evaluate how well the CIELUV space succeeded for our data set, we examined the distribution of the individual matches around the mean match. In Fig. 9 we plot the individual symmetric and asymmetric matches, centered so that the mean for each condition falls at the origin. Thus this plot shows the variability of the individual memory matches. Each of the top three panels plots a single cross section of the three-dimensional cloud of matches in the CIELUV space. The bottom panels show the same data in cone coordinates. The CIELUV transformation greatly improves the homogeneity of the distributions. In Fig. 10 we plot the centered individual matches as a function of the mean match. Each of the top three panels shows such a plot for one of the L^*, u^*, or v^* coordinates. The bottom panels show the same data in cone coordinates. When the data are plotted in cone coordinates, the variability of the matches depends on the mean match. The CIELUV transformation essentially eliminates this dependence.

We use the CIELUV representation only as a perceptually meaningful error metric to evaluate the quality of our

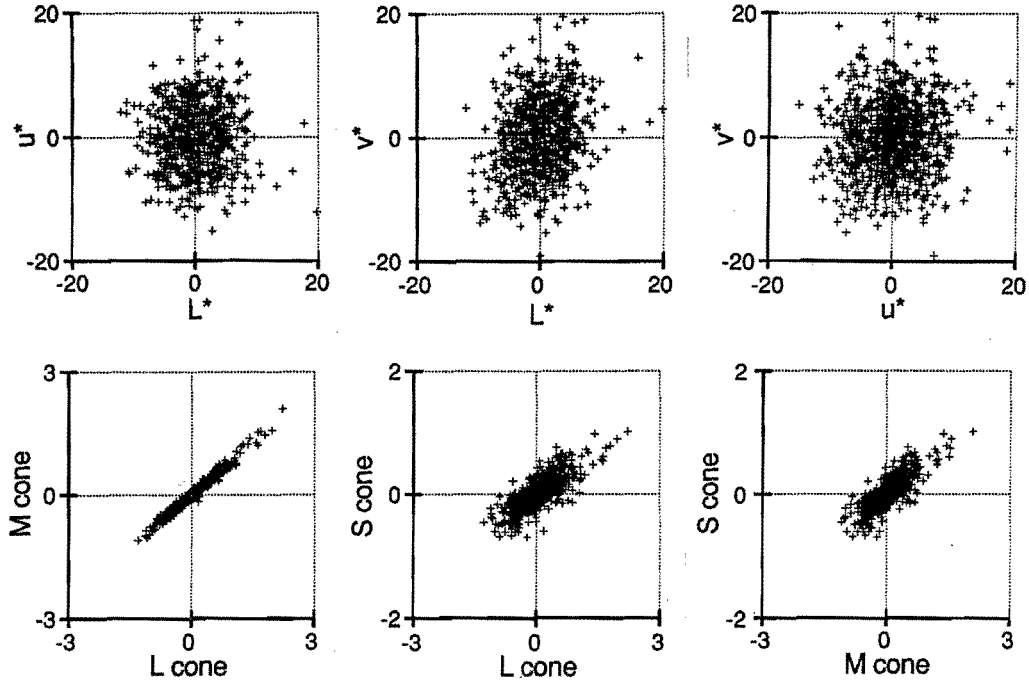

Fig. 9. Scatter of individual matches around the mean match. The top panels show the scatter in CIELUV coordinates; the bottom panels show the scatter in cone coordinates.

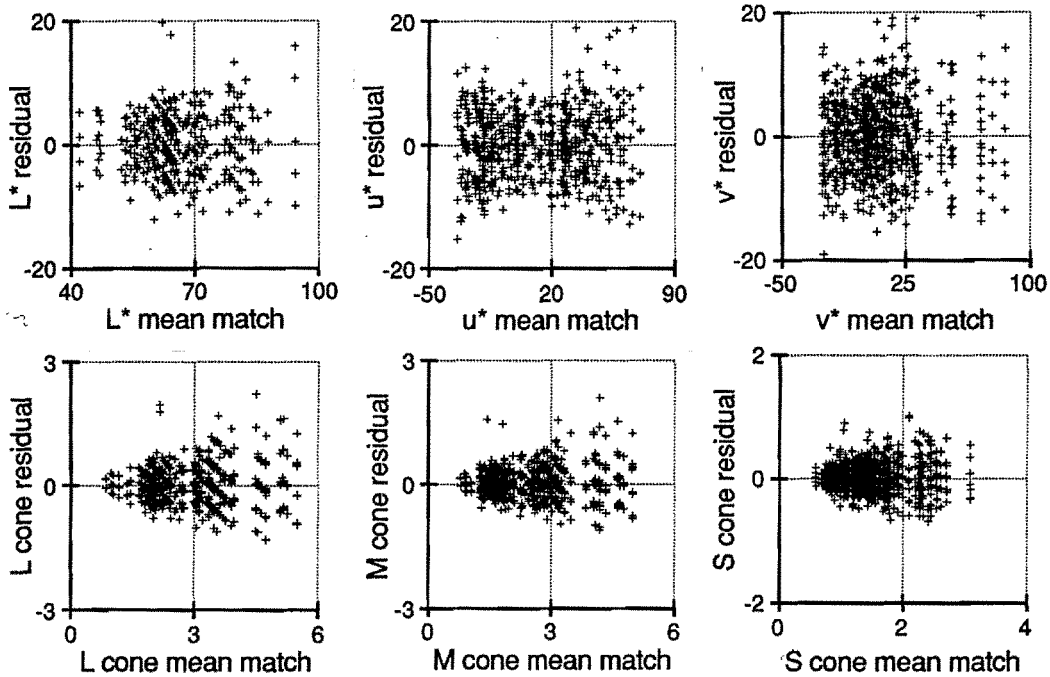

Fig. 10. Scatter of individual matches as a function of the mean match. The top panels show the scatter in CIELUV coordinates; the bottom panels show the scatter in cone coordinates.

model fits. The models themselves are formulated in terms of cone coordinates and do not rely on the CIELUV transformations.

Some authors have suggested that the CIELUV representation, which includes a normalization for the ambient illumination, might serve as a color appearance model for asymmetric color matching.[58,59] Were this true, the CIELUV representation of the standard object and the asymmetric color match would be the same. As we describe more fully elsewhere, the difference between the CIELUV representation of the standard object and the measured asymmetric color match is quite large.[60] Using the CIELUV transformation to predict the asymmetric matches fares no better than using the untransformed cone coordinates of the standard object (no-model condition).

DISCUSSION

Models of Color Appearance

We measured and analyzed asymmetric matches, using a variety of simulated objects and illuminants. We exam-

ined a group of simple models (Figs. 3 and 4) that predict the matches as a function of both independent variables. For the modest range of contrast we could obtain with our CRT monitor, we found that the asymmetric color matches can be described by a diagonal linear transformation of the standard object's cone coordinates. Further, we found that the elements of the diagonal transformation are linearly related to the change in the simulated illuminant.

All three of our models have the desirable property that a relatively small number of measurements determine the model parameters. When the functional form of the transformation is affine, linear, or diagonal, asymmetric matches for a small number of standard objects permit the prediction of asymmetric matches for any standard object. When the principle of illuminant linearity holds, asymmetric matches made for a group of illuminant changes permit the prediction of asymmetric matches for any linear combination of these illuminant changes. This property is especially useful because Judd *et al.*[8] showed that the variation in natural daylight can be described by a linear combination of as few as four basis illuminant changes.

At first, the simplicity of our models for asymmetric matching may appear astonishing compared with the complexity of some current models of color appearance.[61,62] Complete color appearance models must cope with a wide variety of phenomena beyond asymmetric matches, in particular, perceptual naming and scaling. By studying asymmetric matches, we can separate the effect of viewing context on color appearance from these broader phenomena. Just as the basic color-matching experiment reveals an important early linearity, we think that our asymmetric color-matching experiments reveal linearities before the site of complex perceptual judgments. The effect of the illuminant on color appearance may be mediated by early visual mechanisms.

Although an understanding of asymmetric color matches does not provide a complete theory of color appearance, it does greatly simplify the development of such a theory. Suppose that we can establish general rules to predict appearance matches across viewing contexts. Then perceptual naming and scaling experiments need be examined for only a single viewing context. The theory of asymmetric matching would permit generalization of the results to other viewing contexts.

This approach to simplifying color appearance theories is implicit in Hunt's[61] model of color appearance [see Eq. (5) of his paper]. At an early point in the model calculations, cone photopigment absorption rates are mapped to new values corrected for the observer's adapted state. Over modest contrast ranges, such as we could obtain on our television monitors, the mapping used by Hunt is close to the diagonal model. In his theory, equal values at this early stage in the calculation lead to equal color appearance descriptors. To predict asymmetric color matches, most of the complex calculations in Hunt's model can be ignored.

Another striking simplicity in our data is that the full affine model does not provide a substantially better fit than the reduced linear or diagonal model (see Fig. 5). Jameson and Hurvich[52,53] and, subsequently, Walraven[54] and Shevell[55] emphasized that in general the effect of adaptation on color appearance cannot be explained by gain changes alone. In addition to gain changes, a second additive process is required for the explanation of a variety of color appearance phenomena. It is exactly this additive process that differentiates our affine model from our reduced models.

Jameson and Hurvich[53] attribute the additive term of the two-process model to the effects of simultaneous contrast. When the experimental stimuli are isolated tests presented on uniform backgrounds, it is not possible to separate the effects of simultaneous contrast from the effects of adaptation. Our experimental procedure was designed to measure the effect of adaptation to the illuminant. We varied the location of the test and the identity of the context objects from trial to trial to randomize against simultaneous contrast effects. That we do not require an additive term to model our asymmetric matching data suggests that changing the illuminant affects only the multiplicative stage of adaptation, while the additive term remains constant across changes of illumination.

A complete theory of asymmetric matching must include a description of the effects of contrast as well as the effects of illumination. An intriguing hypothesis suggested by our results is that these two processes can be studied separately. If true, this hypothesis would greatly reduce the number of experimental conditions that need to be examined to develop such a theory.

Mechanisms of Adaptation

Our models can be easily understood in terms of visual mechanisms. In the diagonal model, the adapted state is determined only by three gain factors that modulate signals from the three cone classes before these signals are combined by higher-level opponent mechanisms. This hypothesis about adaptation is due to von Kries[3] and is the form proposed by Jameson and Hurvich[52,53] for the first stage of their two-process model. The more general linear and affine models differ from the diagonal model by permitting the signals for each cone type to be modulated independently in different opponent channels. The diagonal model fits our data essentially as well as the linear and affine models, suggesting that for our conditions the gain changes occur before the combination of signals from separate cone classes.

Although the diagonal model implies that the site of the gain changes must be early, it is silent about the source of the signals that regulate the gain. In Fig. 11 we distinguish between two methods of regulating receptor gain. The top of the figure illustrates the simplest idea. According to this model, the gain of the signal from each cone class is regulated by the photopigment absorptions originating entirely within that cone class. This principle is often implied by the term von Kries adaptation and is the central idea of Land's retinex theory.[63-65]

At least two types of data argue against the model of gain regulation shown in the top of Fig. 11. First, field mixture experiments have shown that sensitivity to a test signal initiated in, say, the L cones can be influenced by the signals from the M and the S cones. Similarly, sensitivity to a test signal initiated in the S cones can be influenced by signals from the L and M cones.[66-72] Second, Werner and Walraven[73] measured achromatic loci for small tests presented on a variety of spectral backgrounds. They found that they could account for their

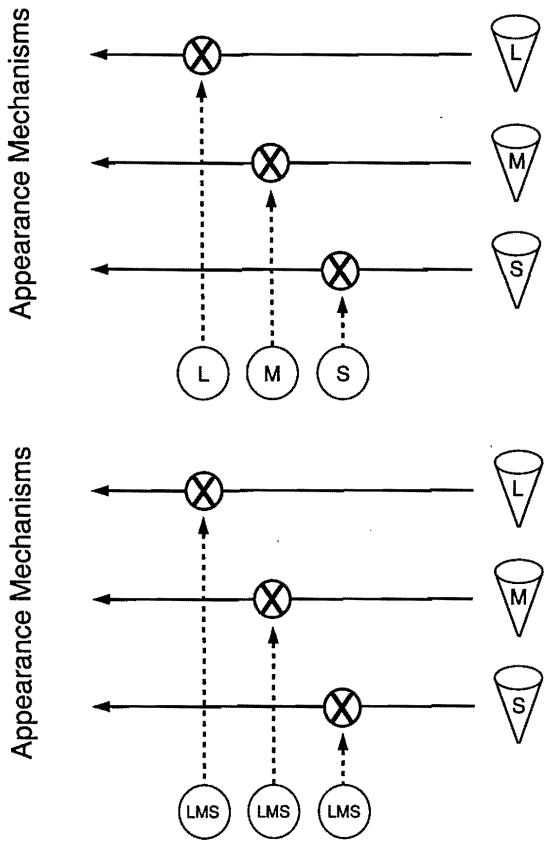

Fig. 11. Control of the elements of the diagonal matrix (i.e., the receptoral gain mechanisms) may be derived in a variety of ways. The diagonal elements may be determined only by the photopigment absorptions within the corresponding cone class, as illustrated at the top of the figure. Alternatively, the gains may be determined by a signal pooled from several classes of cones. This idea is illustrated at the bottom of the figure. Our data do not distinguish between these two hypotheses. In both diagrams, the circled ×'s depict multiplicative regulation between the cone responses and higher-level appearance mechanisms. The vertical arrows indicate the source of the signals that set the multiplicative gain.

data by assuming that adaptation is described by a diagonal linear transformation. They found, however, that the diagonal element describing the S cone sensitivity depends on the response of the L and the M cones to the background. Similarly, Shevell and Humanski[74] showed that the red–green color appearance of a test light seen only by the L and the M cones is modulated by changes in a background field that are visible only to the S cones. Thus both sensitivity and appearance data argue against the simple model of cone sensitivity regulation. Taken together, these experiments suggest that such regulation is mediated by mechanisms that receive input from multiple cone classes. The bottom of Fig. 11 is a schematic for this model of gain control.

Because our experimental manipulations involved illuminant changes, we cannot use our data to distinguish sharply between the two hypotheses. Although our experiments do not reveal how different cone classes combine to regulate gain, the principle of illuminant linearity does provide important information about this regulation. Illuminant linearity implies that the regulation mechanisms linearly combine signals across cone classes and across space. Our results suggest that future investigations can employ linear-systems techniques to probe the nature of these mechanisms.

APPENDIX A

Formal Description of Models

Preliminaries. This appendix provides a formal description of our three models. Let $\mathbf{r}_s$ be a three-dimensional column vector representing the cone coordinates of the standard object rendered under the standard illuminant. Similarly, let $\mathbf{r}_m$ represent the cone coordinates of the mean asymmetric match set under the test illuminant. We define the match change as $\Delta\mathbf{r} = \mathbf{r}_m - \mathbf{r}_s$. Let $\mathbf{e}_s$ be an m-dimensional column vector representing the standard illuminant. The elements of $\mathbf{e}_s$ are the weights on the m linear model basis functions with respect to which the illuminants are represented. For our experiment $m = 2$. Similarly, let $\mathbf{e}_t$ represent the test illuminant. We define the illuminant change as $\Delta\mathbf{e} = \mathbf{e}_t - \mathbf{e}_s$. We formulate our models to predict $\Delta\mathbf{r}$ as a function of $\mathbf{r}_s$ and $\Delta\mathbf{e}$ when $\mathbf{e}_s$ is held fixed. This formulation simplifies the description of the illuminant linearity property. The measured mean asymmetric match $\mathbf{r}_m$ can be recovered from the match change by adding $\mathbf{r}_s$. At the end of this appendix we develop a generalization of the models to the case in which both $\mathbf{e}_s$ and $\mathbf{e}_t$ are permitted to vary.

Functional Form of the Transformation. For any fixed illuminant change $\Delta\mathbf{e}$, the models have the general form

$$\Delta\mathbf{r} = \mathbf{T}_{\Delta\mathbf{e}}\mathbf{r}_s + \mathbf{a}_{\Delta\mathbf{e}}, \tag{A1}$$

where $\mathbf{T}_{\Delta\mathbf{e}}$ is a 3×3 matrix that depends on $\Delta\mathbf{e}$ and $\mathbf{a}_{\Delta\mathbf{e}}$ is a three-dimensional column vector that depends on $\Delta\mathbf{e}$. In the affine model, the nine elements of $\mathbf{T}_{\Delta\mathbf{e}}$ and the three elements of $\mathbf{a}_{\Delta\mathbf{e}}$ are permitted to vary. The linear model is a special case of the affine model in which the elements of $\mathbf{a}_{\Delta\mathbf{e}}$ are constrained to be zero. The diagonal model is a special case of the linear model in which the off-diagonal elements of $\mathbf{T}_{\Delta\mathbf{e}}$ are constrained to be zero.

Illuminant Linearity. Equation (A1) specifies the general functional form of the transformation that predicts the match change. To complete the description of our models, we must specify how $\mathbf{T}_{\Delta\mathbf{e}}$ and $\mathbf{a}_{\Delta\mathbf{e}}$ depend on $\Delta\mathbf{e}$. We impose the illuminant linearity property. Let $\Delta e_i, i = 1, \ldots, m$ be the m elements of $\Delta\mathbf{e}$. We require that

$$\mathbf{T}_{\Delta\mathbf{e}} = \sum_{i=1}^{m} \Delta e_i \mathbf{T}_i, \tag{A2}$$

$$\mathbf{a}_{\Delta\mathbf{e}} = \sum_{i=1}^{m} \Delta e_i \mathbf{a}_i, \tag{A3}$$

where the $\mathbf{T}_i$ are 3×3 matrices and the $\mathbf{a}_i$ are three-dimensional vectors. The elements of the m matrices $\mathbf{T}_i$ and vectors $\mathbf{a}_i$ are the model parameters. For our case of $m = 2$, the affine model has $24 = (2 \times 9) + (2 \times 3)$ parameters, the linear model has $18 = (2 \times 9)$ parameters, and the diagonal model has $6 = (2 \times 3)$ parameters. Once these parameters are specified, Eqs. (A1)–(A3) predict the match change for any standard object and test illuminant.

Table 1. Experimental Stimuli: Cone Coordinates[a]

Standard Object	L Cone Coordinate	M Cone Coordinate	S Cone Coordinate
A	2.25	1.59	0.84
B	1.87	1.53	0.87
C	1.97	1.83	1.33
D	0.90	0.82	0.58
E	3.71	3.31	1.61
F	3.69	3.00	1.89
G	2.18	1.70	0.71
H	1.28	0.95	0.75
I	2.89	2.11	1.15
J	0.93	0.78	0.64
K	1.98	1.80	1.43
L	3.71	3.31	1.61
M	3.22	2.78	1.30
N	1.83	1.59	1.00
O	3.67	3.05	2.06
P	2.50	2.21	1.82
Q	1.99	1.32	0.94
R	2.63	1.98	1.11
S	3.59	2.82	1.35

[a]Cone coordinates of the standard objects when rendered under the standard illumination.

Fitting the Models

It is possible to reexpress the models described by Eqs. (A1)–(A3) by using a single linear equation. Let the m vectors $\mathbf{r}_{si}, i = 1, \ldots, m$ be given by $\mathbf{r}_{si} = \Delta e_i \mathbf{r}_s$. Form the $4m$-dimensional column vector $\mathbf{x}$ by row stacking the m three-dimensional column vectors $\mathbf{r}_{si}$ and the m-dimensional column vector $\Delta\mathbf{e}$. The vector $\mathbf{x}$ is completely determined by $\mathbf{r}_s$ and $\Delta\mathbf{e}$. The affine model expressed by Eqs. (A1)–(A3) is equivalent to

$$\Delta\mathbf{r} = \mathbf{T}\mathbf{x}, \tag{A4}$$

where $\mathbf{T}$ is a $3 \times 4m$ dimensional matrix formed by column stacking the matrices $\mathbf{T}_i$ and the vectors $\mathbf{a}_j$:

$$\mathbf{T} = [\mathbf{T}_1 \vdots \ldots \vdots \mathbf{T}_m \vdots \ldots \vdots \mathbf{a}_m]. \tag{A5}$$

The equivalence between the two formulations can be established by explicitly expanding the summations implicit in the two sets of matrix equations. Similar reexpressions are possible for both the linear and the diagonal models, although we do not describe them here.

When the models are expressed as a single system of linear equations [as in Eq. (A4)], it is possible to determine the parameters of the model (the elements of $\mathbf{T}$) by using standard multiple regression. The regression procedure minimizes the mean-square difference between the measured and the predicted match changes. In fitting the models to the data, we began with the regression fit and then used the STEPIT parameter search program[57] to adjust the parameters to minimize the mean-square CIELUV difference ΔE_{uv}^* between the measured and the predicted asymmetric matches.[75]

Relation to Other Models

Our diagonal model is closely related to a strong form of von Kries adaptation in which the gain of each cone class is taken to be inversely proportional to some spatial and temporal average of the quantal absorptions in that class. Let the numbers $w_{si}, i = 1, \ldots, 3$ represent this weighted average for each of the three cone classes under the standard illuminant, and, similarly, let $w_{ti}, i = 1, \ldots, 3$ do so under the test illuminant. Let $\mathbf{W}_s$ be a 3×3 diagonal matrix whose diagonal elements are the w_{si} and similarly for $\mathbf{W}_t$. Under the assumption that the only change with adaptation is a gain change for each cone class, we can predict asymmetric matches through the equation

$$\mathbf{W}_s^{-1}\mathbf{r} = \mathbf{W}_t^{-1}(\mathbf{r} + \Delta\mathbf{r}), \tag{A6}$$

which implies that

$$\begin{aligned}\Delta\mathbf{r} &= (\mathbf{W}_t\mathbf{W}_s^{-1} - \mathbf{I})\mathbf{r} \\ &= (\mathbf{W}_t - \mathbf{W}_s)\mathbf{W}_s^{-1}\mathbf{r} \\ &= \mathbf{T}_{\Delta\mathbf{e}}\mathbf{r},\end{aligned} \tag{A7}$$

where $\mathbf{T}_{\Delta\mathbf{e}} = (\mathbf{W}_t - \mathbf{W}_s)\mathbf{W}_s^{-1}$. Equation (A7) is a special case of our diagonal model in which the elements of $\mathbf{T}_{\Delta\mathbf{e}}$ are determined by the average quantal absorptions within each cone class under each illuminant. When the standard illuminant is held fixed, the elements of $\mathbf{T}_{\Delta\mathbf{e}}$ depend linearly on the illuminant change. Our diagonal model is more general than this form of the von Kries adaptation because it allows for more complex gain regulation mechanisms. In particular, it allows for the possibility that gain regulation mechanisms combine information across cone classes.

A similar argument shows that the model of Werner and Walraven[73] is a special case of our affine model with one important difference: our illuminant linearity property precludes the incorporation of Stiles's $1/\zeta(x)$ function into the relation between the π-mechanism responses and the

Table 2. Experimental Stimuli: Illuminants[a]

Illuminant	x Chromaticity	y Chromaticity	Luminance	Weight 1	Weight 2
S	0.34	0.35	42.81	5.97×10^{-8}	-5.44×10^{-8}
T1	0.27	0.29	35.57	4.77×10^{-8}	6.30×10^{-8}
T2	0.31	0.32	78.39	1.07×10^{-7}	8.55×10^{-9}
T3	0.34	0.35	85.63	1.19×10^{-7}	-1.09×10^{-7}
T4	0.27	0.29	71.14	9.53×10^{-8}	1.26×10^{-7}
T5	0.41	0.42	100.11	1.44×10^{-7}	-3.44×10^{-7}
T6	0.21	0.22	28.33	3.56×10^{-8}	1.80×10^{-7}

[a]Each of our illuminants is specified by its CIE x and y chromaticity coordinates and luminance in candelas per square meter. Also given are the weights that are used to construct the illuminant as a linear combination of the published mean and first characteristic vector of Judd *et al.*[8] The units of the resulting spectral power distributions are milliwatts per square centimeter nanometer steradian.

Table 3. Experimental Data[a]

Standard Object	Test Illuminant	Subject	Symmetric Match			Asymmetric Match		
			L	M	S	L	M	S
A	T1	DB	2.19	1.53	0.82	2.13	1.56	1.12
A	T2	DB	2.32	1.63	0.85	3.37	2.42	1.53
A	T3	DB	2.43	1.71	0.91	3.85	2.73	1.50
A	T4	DB	2.13	1.46	0.76	3.18	2.33	1.65
A	T5	DB	2.12	1.48	0.79	3.89	2.66	1.09
A	T6	DB	2.00	1.39	0.74	1.91	1.47	1.13
H	T1	DB	1.67	1.24	0.99	1.17	0.92	0.94
I	T1	DB	2.66	1.94	1.10	2.74	2.08	1.49
J	T1	DB	1.04	0.89	0.68	0.85	0.77	0.81
K	T1	DB	1.83	1.68	1.28	1.83	1.76	1.68
L	T1	DB	3.36	2.98	1.52	3.49	3.23	1.99
M	T1	DB	3.12	2.73	1.27	3.13	2.83	1.60
N	T1	DB	1.81	1.56	1.07	1.72	1.56	1.32
O	T1	DB	3.40	2.82	1.93	3.45	2.97	2.45
P	T1	DB	2.71	2.43	1.92	2.41	2.28	2.19
Q	T1	DB	2.21	1.49	1.05	1.97	1.37	1.19
R	T1	DB	2.36	1.74	0.92	2.44	1.87	1.19
S	T1	DB	3.47	2.68	1.24	3.21	2.59	1.47
A	T1	SE	2.26	1.65	0.91	2.30	1.76	1.29
A	T2	SE	2.23	1.62	0.89	3.08	2.30	1.57
A	T3	SE	2.09	1.53	0.86	3.06	2.23	1.28
A	T3	SE	2.11	1.51	0.83	3.49	2.55	1.47
A	T4	SE	2.57	1.90	1.03	3.49	2.66	1.80
A	T5	SE	2.38	1.71	0.89	3.76	2.65	1.19
A	T6	SE	2.38	1.70	0.95	2.40	1.85	1.42
B	T1	SE	2.00	1.68	0.98	2.08	1.79	1.22
B	T1	SE	1.77	1.47	0.85	1.81	1.56	1.11
B	T2	SE	2.17	1.80	1.04	3.38	2.84	1.93
B	T3	SE	1.95	1.61	0.93	3.06	2.53	1.49
B	T4	SE	1.78	1.46	0.84	2.97	2.58	1.93
B	T5	SE	2.05	1.69	1.05	3.49	2.77	1.29
B	T6	SE	1.92	1.59	0.91	1.74	1.61	1.27
C	T1	SE	1.87	1.68	1.21	1.72	1.64	1.43
C	T2	SE	1.85	1.71	1.24	3.07	2.84	2.28
C	T3	SE	2.00	1.85	1.37	3.36	3.11	2.31
D	T2	SE	0.98	0.88	0.59	1.45	1.33	1.06
H	T2	SE	1.38	1.03	0.77	1.94	1.50	1.34
I	T2	SE	2.76	2.05	1.18	3.97	3.01	1.85
M	T2	SE	3.13	2.72	1.34	4.74	4.19	2.28
P	T2	SE	2.54	2.24	1.78	3.62	3.26	3.08
Q	T2	SE	2.23	1.55	1.01	2.70	1.87	1.47
S	T2	SE	3.74	2.92	1.41	5.08	4.03	2.25
E	T2	SE	3.58	3.17	1.46	5.17	4.62	2.45
F	T2	SE	3.55	2.90	1.70	4.62	3.85	2.69
G	T2	SE	2.08	1.63	0.75	3.13	2.51	1.40
K	T1	KH	2.01	1.83	1.50	1.92	1.84	1.75
K	T2	KH	2.26	2.08	1.68	3.18	2.97	2.60
K	T3	KH	2.01	1.84	1.48	3.04	2.78	2.27
L	T1	KH	4.55	4.08	1.77	4.49	4.18	2.10
L	T2	KH	3.64	3.32	1.54	4.73	4.33	2.32
L	T3	KH	3.47	3.13	1.43	5.49	4.98	2.40
Q	T1	KH	1.99	1.25	0.82	2.03	1.34	1.07
Q	T2	KH	2.06	1.36	0.93	3.35	2.26	1.75
Q	T3	KH	2.02	1.28	0.98	3.03	1.98	1.48
K	T1	LL	2.16	1.98	1.52	1.83	1.76	1.71
L	T1	LL	3.70	3.33	1.63	3.34	3.14	1.85
L	T2	LL	3.56	3.21	1.50	5.26	4.77	2.53
Q	T2	LL	2.23	1.46	0.98	2.98	2.06	1.62
L	T1	DW	3.90	3.48	1.55	3.30	3.08	1.74
L	T2	DW	3.42	3.11	1.55	5.14	4.67	2.54
Q	T1	DW	2.17	1.42	1.06	1.92	1.30	1.20

[a]Each row specifies the results for one experimental condition. The standard object and test illuminant designators refer to Tables 1 and 2.

Table 4. Parameters of the Diagonal Model That Best Fits the Data[a]

Diagonal Matrix Number	L Cone Entry	M Cone Entry	S Cone Entry
1	8.76×10^6	9.10×10^6	1.12×10^7
2	3.92×10^5	7.51×10^5	2.64×10^6

[a]Each row provides the diagonal elements for one of the two diagonal matrices $\mathbf{T}_i$ that are required for specification of the parameters of the diagonal model. For any illuminant change, these two matrices should be combined according to Eq. (A2) to produce the diagonal matrix that predicts the match changes. For each illuminant change the appropriate values of Δe_1 and Δe_2 may be found by subtracting the standard and the test illuminant linear model weights given in Table 2. For our entire data set, the rms prediction error (in cone coordinates) of this diagonal model is 0.235.

transformation parameters. We do not require this nonlinearity in order to fit our data.

Our models are also related to computational models of color constancy. A visual system using the algorithms of Buchsbaum[9] or of Maloney and Wandell[10] to extract color-constant surface descriptors would produce asymmetric matches consistent with our linear model. These algorithms show that, when appropriate linear models constrain the surface reflectance functions and illuminant spectral power distributions, color-constant descriptors can be obtained from cone coordinates by a linear equation of the form $\mathbf{s} = \mathbf{L}_e^{-1}\mathbf{r}$, where $\mathbf{s}$ is a three-dimensional vector of color descriptors and $\mathbf{L}_e$ is a 3×3 matrix whose elements depend linearly on the illuminant. If the descriptors $\mathbf{s}$ mediate color appearance, then we can derive the relation $\Delta\mathbf{r} = (\mathbf{L}_{e_t} - \mathbf{L}_{e_s})\mathbf{L}_{e_s}^{-1}\mathbf{r}$. This clearly has the functional form of our linear model. Since the elements of the $\mathbf{L}_e$ depend linearly on the illuminant, the transformation $\mathbf{T}_{\Delta e} = (\mathbf{L}_{e_t} - \mathbf{L}_{e_s})\mathbf{L}_{e_s}^{-1}$ also satisfies the illuminant linearity property.

Extending the Models

We developed our models on the assumption that the standard illuminant $\mathbf{e}_s$ is held fixed. This assumption holds for our data set. When both the standard illuminant and the test illuminants are permitted to vary, there are two important empirical properties of asymmetric matching that must hold if color appearance is well defined. These are the properties of symmetry and transitivity.[76] Together, symmetry and transitivity ensure that conclusions about the identity of appearance are consistent across different choices of measurement conditions. Symmetry and transitivity are typically assumed to hold for asymmetric matching. Although we have not performed extensive checks, pilot data indicate that these two properties do indeed hold for our measurement procedure.

Let $\mathbf{e}_a$, $\mathbf{e}_b$, and $\mathbf{e}_c$ be three illuminants, and let the expression $\mathbf{r} \sim_{a\to b} \mathbf{r}'$ denote that the asymmetric match for an object with cone coordinates $\mathbf{r}$ (when illuminated by $\mathbf{e}_a$) across the illuminant change from $\mathbf{e}_a$ to $\mathbf{e}_b$ is an object with cone coordinates $\mathbf{r}'$ (when illuminated by $\mathbf{e}_b$). The symmetry property is that if $\mathbf{r} \sim_{a\to b} \mathbf{r}'$ then $\mathbf{r}' \sim_{b\to a} \mathbf{r}$. The transitivity property is that if $\mathbf{r} \sim_{a\to b} \mathbf{r}'$ and $\mathbf{r}' \sim_{b\to c} \mathbf{r}''$ then $\mathbf{r} \sim_{a\to c} \mathbf{r}''$.

Together symmetry and transitivity allow us to predict asymmetric matches when the standard illuminant is $\mathbf{e}_b$ from measured asymmetric matches when the standard illuminant is $\mathbf{e}_a$. For any test illuminant $\mathbf{e}_c$, we first use the symmetry property and the relation $\sim_{a\to b}$ to derive the relation $\sim_{b\to a}$. We then use the transitivity property, the relation $\sim_{b\to a}$, and the relation $\sim_{a\to c}$ to derive the desired relation $\sim_{b\to c}$. Thus, when symmetry and transitivity hold, no loss of generality results from making measurements with respect to a fixed standard illuminant.[77]

It is possible to carry out the above derivation process explicitly for each of our three models. The results of these derivations allow us to show that, when any of our models describes asymmetric matches measured with respect to standard illuminant $\mathbf{e}_a$, it also describes asymmetric matches with respect to any other standard illuminant. For example, suppose that the affine model describes asymmetric matches when the standard illuminant is $\mathbf{e}_a$. Let the matrix $\mathbf{T}_{ab}$ and the vector $\mathbf{a}_{ab}$ describe the affine transformation when the test illuminant is $\mathbf{e}_b$ and similarly for $\mathbf{T}_{ac}$ and $\mathbf{a}_{ac}$. Symmetry and transitivity then allow us to show that asymmetric matches when the standard illuminant is $\mathbf{e}_b$ and the test illuminant is $\mathbf{e}_c$ are described by

$$\Delta\mathbf{r} = \mathbf{T}_{bc}\mathbf{r} + \mathbf{a}_{bc}, \tag{A8}$$

where $\mathbf{T}_{bc} = (\mathbf{T}_{ac} - \mathbf{T}_{ab})(\mathbf{T}_{ab} + \mathbf{I})^{-1}$, $\mathbf{a}_{bc} = (\mathbf{a}_{ac} - \mathbf{a}_{ab}) - (\mathbf{T}_{ac} - \mathbf{T}_{ab})(\mathbf{T}_{ab} + \mathbf{I})^{-1}(\mathbf{a}_{ab})$, and $\mathbf{I}$ is the identity matrix. Consideration of the form of $\mathbf{T}_{bc}$ and $\mathbf{a}_{bc}$ shows that illuminant linearity also holds with respect to standard illuminant $\mathbf{e}_b$.

APPENDIX B

This appendix consists of four tables. Tables 1 and 2 specify our experimental stimuli. Table 1 provides the cone coordinates of the standard objects when they are rendered under the standard illumination. Table 2 specifies each of our illuminants. Table 3 presents our experimental data. Table 4 gives the parameters of the diagonal model that best fits our data. Each row provides the diagonal elements for one of the two diagonal matrices $\mathbf{T}_i$ that are required for specification of the parameters of the diagonal model (see Appendix A). For any illuminant change, these two matrices should be combined according to Eq. (A2) to produce the diagonal matrix $\mathbf{T}_{\Delta e}$ that predicts the match changes.

ACKNOWLEDGMENTS

We thank A. Ahumada, E. J. Chichilnisky, K. Koh, P. Lennie, D. MacAdam, L. Maloney, J. Nachmias, J. Palmer, M. Pavel, A. Poirson, D. Varner, D. Williams, and the referees for useful discussions or comments on earlier versions of this paper. This research is also described in Brainard's doctoral dissertation.[35] A preliminary report was presented at the Symposium on Electronic Imaging[78] of the SPIE—International Society for Optical Engineering/Society for Imaging Science and Technology. Support was provided by grant 2 RO1 EY03164 from the National Eye Institute, grant NCC 2-307 from the National Aeronautics and Space Administration—Ames Research Center, a National Science Foundation graduate fellowship, and grant 204E from the Cowper Institute.

*Present address, Department of Psychology, University of California, Santa Barbara, Santa Barbara, California 93106.

REFERENCES AND NOTES

1. W. S. Stiles, "Mechanism concepts in colour theory," J. Colour Group **11,** 106–123 (1967) [in *Mechanisms of Colour Vision,* W. S. Stiles, ed. (Academic, London, 1978)].
2. D. Krantz, "A theory of context effects based on cross-context matching," J. Math. Psychol. **5,** 1–48 (1968).
3. J. von Kries, "Influence of adaptation on the effects produced by luminous stimuli," Handb. Physiol. Menschen **3,** 109–282 (1905) [in *Sources of Color Vision,* D. L. MacAdam, ed. (MIT Press, Cambridge, Mass., 1970)].
4. J. Cohen, "Dependency of the spectral reflectance curves of the Munsell color chips," Psychon. Sci. **1,** 369–370 (1964).
5. L. T. Maloney, "Evaluation of linear models of surface spectral reflectance with small numbers of parameters," J. Opt. Soc. Am. A **3,** 1673–1683 (1986).
6. J. P. S. Parkkinen, J. Hallikainen, and T. Jaaskelainen, "Characteristic spectra of Munsell colors," J. Opt. Soc. Am. A **6,** 318–322 (1989).
7. T. Jaaskelainen, J. Parkkinen, and S. Toyooka, "A vector-subspace model for color representation," J. Opt. Soc. Am. A **7,** 725–730 (1990).
8. D. B. Judd, D. L. MacAdam, and G. W. Wyszecki, "Spectral distribution of typical daylight as a function of correlated color temperature," J. Opt. Soc. Am. **54,** 1031–1040 (1964).
9. G. Buchsbaum, "A spatial processor model for object color perception," J. Franklin Inst. **310,** 1–26 (1980).
10. L. T. Maloney and B. Wandell, "Color constancy: a method for recovering surface spectral reflectance," J. Opt. Soc. Am. A **3,** 29–33 (1986).
11. D. H. Brainard and B. A. Wandell, "A bilinear model of the illuminant's effect on color appearance," in *Computational Models of Visual Processing,* J. A. Movshon and M. S. Landy, eds. (MIT Press, Cambridge, Mass., 1991).
12. L. Arend and A. Reeves, "Simultaneous color constancy," J. Opt. Soc. Am. A **3,** 1743–1751 (1986).
13. R. W. G. Hunt, "The effects of daylight and tungsten light-adaptation on color perception," J. Opt. Soc. Am. **40,** 336–371 (1950).
14. D. Jameson, L. M. Hurvich, and F. D. Varner, "Receptoral and postreceptoral visual processes in recovery from chromatic adaptation," Proc. Natl. Acad. Sci. USA **76,** 3034–3038 (1979).
15. S. J. Ahn, "Studies of adaptation in the luminance and chromatic channels," Ph.D. dissertation (University of California, San Diego, La Jolla, Calif., 1990).
16. M. D. Fairchild, "Chromatic adaptation and color appearance," Ph.D. dissertation (University of Rochester, Rochester, N.Y., 1990).
17. M. Hayhoe, P. Wenderoth, E. Lynch, and D. H. Brainard, "Adaptation mechanisms in color appearance," Invest. Ophthalmol. Vis. Sci. Suppl. **32,** 1023 (1991).
18. H. Helson and V. B. Jeffers, "Fundamental problems in color vision. II. Hue, lightness, and saturation of selective samples in chromatic illumination," J. Exp. Psychol. **26,** 1–27 (1940).
19. H. Helson, D. Judd, and M. Warren, "Object-color changes from daylight to incandescent filament illumination," Illum. Eng. **47,** 221–233 (1952).
20. R. W. G. Hunt, "The perception of color in 1 degree fields for different states of adaptation," J. Opt. Soc. Am. **43,** 479–484 (1953).
21. D. Jameson and L. M. Hurvich, "Some quantitative aspects of an opponent-colors theory. I. Chromatic responses and spectral saturation," J. Opt. Soc. Am. **45,** 546–552 (1955).
22. D. L. MacAdam, "Chromatic adaptation," J. Opt. Soc. Am. **46,** 500–512 (1956).
23. R. W. Burnham, R. M. Evans, and S. M. Newhall, "Prediction of color appearance with different adaptation illuminations," J. Opt. Soc. Am. **47,** 35–42 (1957).
24. J. J. McCann, S. P. McKee, and T. H. Taylor, "Quantitative studies in retinex theory: a comparison between theoretical predictions and observer responses to the color Mondrian experiments," Vision Res. **16,** 445–448 (1976).
25. A. Valberg and B. Lange-Malecki, "'Color constancy' in mondrian patterns: a partial cancellation of physical chromaticity shifts by simultaneous contrast," Vision Res. **30,** 371–380 (1990).
26. J. Walraven, T. Benzschawel, and B. Rogowitz, "Chromatic induction: a misdirected attempt at color constancy?" in *Optical Society of America 1988 Annual Meeting,* Vol. 11 of 1988 OSA Technical Digest Series (Optical Society of America, Washington, D.C., 1988), p. 103.
27. K. T. Blackwell and G. Buchsbaum, "Quantitative studies of color constancy," J. Opt. Soc. Am. A **5,** 1772–1780 (1988).
28. A. C. Hurlbert, H. Lee, and H. H. Bulthoff, "Cues to the color of the illuminant," Invest. Ophthalmol. Vis. Sci. Suppl. **30,** 221 (1989).
29. D. H. Brainard, "Calibration of a computer controlled color monitor," Color Res. Appl. **14,** 23–34 (1989).
30. G. W. Meyer, H. E. Rushmeier, M. F. Cohen, D. P. Greenberg, and K. E. Torrance, "An experimental evaluation of computer graphics imagery," Assoc. Comput. Mach. Graphics **5,** 30–50 (1986).
31. D. H. Brainard and B. A. Wandell, "Calibrated processing of image color," Color Res. Appl. **15,** 266–271 (1990).
32. D. H. Brainard and B. A. Wandell, "The color analysis package," Applied Psychology. Lab. Rep. 89-3 (Stanford University, Stanford, Calif., 1989).
33. K. L. Kelly, K. S. Gibson, and D. Nickerson, "Tristimulus specification of the *Munsell Book of Color* from spectrophotometric measurements," J. Opt. Soc. Am. **33,** 355–376 (1943).
34. D. Nickerson, "Spectrophotometric data for a collection of Munsell samples" (U.S. Department of Agriculture, Washington, D.C., 1957; available from Munsell Color Company, Baltimore, Md.).
35. D. H. Brainard, "Understanding the illuminant's effect on color appearance," Ph.D. dissertation (Stanford University, Stanford, Calif., 1989).
36. CIE, "Colorimetry," Publ. 15 (Bureau Central, CIE, Paris, 1971).
37. A. R. Robertson, "The CIE 1976 color-difference formulae," Color Res. Appl. **2,** 7–11 (1977).
38. For this purpose, we used the CIE XYZ tristimulus coordinates of the monitor white point for the conversion to CIELUV values.
39. S. Ishihara, *Tests for Colour-Blindness* (Kanehara Shuppen Company, Ltd., Tokyo, 1977).
40. V. Smith and J. Pokorny, "Spectral sensitivity of the foveal cone photopigments between 400 and 500 nm," Vision Res. **15,** 161–171 (1975).
41. To match the wavelength range and sampling of our phosphor calibration measurements, we obtained these estimates by using Boynton's (Ref. 42, p. 404) formula to transform Judd's[43] modified CIE color-matching functions (Ref. 44, p. 330) at wavelengths between 370 and 730 nm. We then linearly interpolated the result to a sampling resolution of 1 nm. Note that Boynton's published formula contains a typographical error: the contribution from color-matching function $\bar{z}$ to the M cone responsivity should be positive. The luminance (in candelas per square meter but with respect to Judd's[43] modified luminous efficiency function) of a light can be recovered from our reported cone coordinates through $Y = 6.83(0.64L + 0.39M)$. Since the Smith–Pokorny estimates are not an exact linear transformation of the 1931 CIE XYZ color-matching function, we incorporated our measured monitor phosphor spectral power distributions in our color coordinate conversion procedures.
42. R. M. Boynton, *Human Color Vision* (Holt, Rinehart & Winston, New York, 1979).
43. D. B. Judd, *Report of U.S. Secretariat Committee on Colorimetry and Artificial Daylight,* Vol. 1 of CIE Proceedings (Bureau Central, CIE, Paris, 1951), part 7.
44. G. Wyszecki and W. S. Stiles, *Color Science* (Wiley, New York, 1982).
45. D. L. MacAdam, "Visual sensitivities to color differences in daylight," J. Opt. Soc. Am. **32,** 247–274 (1942).
46. W. R. J. Brown and D. L. MacAdam, "Visual sensitivities to combined chromaticity and luminance differences," J. Opt. Soc. Am. **39,** 808–834 (1949).
47. G. Wyszecki, and G. H. Fielder, "New color-matching ellipses," J. Opt. Soc. Am. **61,** 1135–1151 (1971).
48. For this purpose, we used the CIE XYZ tristimulus coordinates of the simulated illuminant at the time a match was set to determine the white point for the conversion to CIELUV values.

49. K. V. Mardia, J. T. Kent, and J. M. Bibby, *Multivariate Analysis* (Academic, New York, 1979).
50. The CIELUV representation was designed so that one unit of ΔE_{uv}^* corresponds to one standard deviation in individual match distribution in a simultaneous matching experiment, equivalent to a d-prime of one. Three ΔE_{uv}^* units are typically taken as a just-noticeable difference in industrial applications [L. D. Silverstein, UCD Sciences, Inc., Scottsdale, Ariz. (personal communication, 1991)].
51. We performed two-tailed t tests on the differences in L^*, u^*, and v^* mean match coordinates. For 48 mean matches from the 24 experimental conditions in which we had repeat measurements between subjects, we found the probability of the observed deviations between subjects' mean matches to be greater than 0.10 for each of the three coordinates.
52. D. Jameson and L. M. Hurvich, "Theory of brightness and color contrast in human vision," Vision Res. **4,** 135–154 (1964).
53. D. Jameson and L. M. Hurvich, "Color adaptation: sensitivity contrast, and afterimages," in *Handbook of Sensory Physiology,* L. M. Hurvich and D. Jameson, eds. (Springer-Verlag, Berlin, 1972).
54. J. Walraven, "Discounting the background—the missing link in the explanation of chromatic induction," Vision Res. **16,** 289–295 (1976).
55. S. K. Shevell, "The dual role of chromatic backgrounds in color perception," Vision Res. **18,** 1649–1661 (1978).
56. C. Ware, and W. B. Cowan, "Changes in perceived color due to chromatic interactions," Vision Res. **22,** 1353–1362 (1982).
57. J. P. Chandler, "STEPIT" (Quantum Chemistry Program Exchange, Department of Chemistry, Indiana University at Bloomington, Ind., 1965).
58. B. J. Lindbloom, "Accurate color reproduction for computer graphics applications," Comput. Graphics **23,** 117–126 (1989).
59. R. J. Motta, "Color encoding computer images—part two," Inf. Disp. **7,** 16–19 (1991).
60. D. H. Brainard and B. A. Wandell, "Evaluation of CIE Luv and CIE Lab as perceptual image representations," Soc. Inf. Disp. Int. Symp. Tech. Dig. **22,** 799–801 (1991).
61. R. W. G. Hunt, "A model of colour vision for predicting color appearance in various viewing conditions," Color Res. Appl. **12,** 297–314 (1987).
62. Y. Nayatani, K. Hashimoto, K. Takahama, and H. Sobagaki, "A non-linear color-appearance model using Estevez–Hunt–Pointer primaries," Color Res. Appl. **12,** 231–242 (1987).
63. E. H. Land and J. J. McCann, "Lightness and retinex theory," J. Opt. Soc. Am. **61,** 1–11 (1971).
64. E. H. Land, "Recent advances in retinex theory and some implications for cortical computations: color vision and the natural image," Proc. Natl. Acad. Sci. USA **80,** 5163–5169 (1983).
65. D. H. Brainard and B. A. Wandell, "Analysis of the retinex theory of color vision," J. Opt. Soc. Am. A **3,** 1651–1661 (1986).
66. J. D. Mollon and P. G. Polden, "An anomaly in the response of the eye to light of short wavelengths," Philos. Trans. R. Soc. London Ser. B **278,** 207–240 (1977).
67. P. G. Polden and J. D. Mollon, "Reversed effect of adapting stimuli on visual sensitivity," Proc. R. Soc. London Ser. B **210,** 235–272 (1980).
68. E. N. Pugh, "The nature of the π_1 mechanism of W. S. Stiles," J. Physiol. **257,** 713–747 (1976).
69. E. N. Pugh and J. D. Mollon, "A theory of the π_1 and π_3 colour mechanisms of Stiles," Vision Res. **19,** 293–312 (1979).
70. C. E. Sternheim, I. C. F. Stromeyer, and L. Spillmann, "Increment thresholds: sensitization produced by hue differences," in *Visual Psychophysics and Physiology,* J. Armington, J. Krauskopf, and B. R. Wooten, eds. (Academic, New York, 1978).
71. B. A. Wandell and E. N. Pugh, "A field-additive pathway detects brief-duration, long-wavelength incremental flashes," Vision Res. **20,** 613–624 (1980).
72. B. A. Wandell and E. N. Pugh, "Detection of long-duration, long-wavelength incremental flashes by a chromatically coded pathway," Vision Res. **20,** 625–636 (1980).
73. J. S. Werner and J. Walraven, "Effect of chromatic adaptation on the achromatic locus: the role of contrast, luminance and background color," Vision Res. **22,** 929–944 (1982).
74. S. K. Shevell and R. A. Humanski, "Color perception under chromatic adaptation: red/green equilibria with adapted short-wavelength-sensitive cones," Vision Res. **28,** 1345–1356 (1988).
75. The STEPIT routine can simultaneously search for optimal values for 20 parameters. To fit the affine model, which has 24 parameters, we called the STEPIT routine repeatedly on subsets of the full parameter set. For all the STEPIT fits, we tried a number of different initial conditions.
76. G. Wyszecki, "Color appearance," in *Handbook of Perception,* K. Boff, L. Kaufman, and J. P. Thomas, eds. (Wiley, New York, 1986).
77. Strictly speaking, this argument also requires the assumption that all objects seen under illuminant $\mathbf{e}_b$ have a satisfactory asymmetric match under illuminant $\mathbf{e}_a$.
78. D. H. Brainard and B. A. Wandell, "The effect of the illuminant on color appearance," in *Perceiving, Measuring, and Using Color,* M. H. Brill, ed., Proc. Soc. Photo-Opt. Instrum. Eng. **1250,** 119–130 (1990).